Wetting of underliquid systems

by

Kumari Trinavee

A thesis
presented to the University of Waterloo
in fulfillment of the
thesis requirement for the degree of
Master of Applied Science
in
Mechanical and Mechatronics Engineering

Waterloo, Ontario, Canada, 2019

Examining Committee Membership

The following served on the Examining Committee for this thesis.

Supervisor:	Sushanta K. Mitra Professor, Dept. of Mechanical and Mechatronics Engineering, University of Waterloo
Examiner (s):	Carolyn Ren Professor, Dept. of Mechanical and Mechatronics Engineering, University of Waterloo
	Boxin Zhao Professor, Dept. Chemical Engineering, University of Waterloo

Author's Declaration

I hereby declare that I am the sole author of this thesis. This is a true copy of the thesis, including any required final revisions, as accepted by my examiners.

I understand that my thesis may be made electronically available to the public.

Abstract

Wetting studies can be tracked back over the last few decades due to its applications in the development of water repellent (superhydrophobic), oil repellent (superoleophobic) surfaces. Despite the fact that these surfaces are well explored for air medium (inviscid), still the subject remains an emerging and challenging field due to the dearth of fundamental studies of wetting in surrounding viscous medium. Analyzing the interaction of a liquid droplet with a surface when kept in another liquid medium is vital for evolving applications in aquatic environment, oil-spillage, designing functional interfaces etc. The present study identifies and addresses a systematic study of two different underliquid systems : oil (drop) in water (surrounding medium) and water (drop) in oil (surrounding medium) with two different substrates viz., Poly (methyl methacrylate) PMMA and glass. Conventional theories namely, Young's equation and Owens-Wendt approach were corroborated with experimentally observed results. It was found that that experimental values vary largely with the conventional theoretical model for water (drop) in oil (viscous surrounding medium) on PMMA substrate. However, oil (drop) in water medium on PMMA substrate do not show such an anomaly. Therefore we hypothesized that a thin oil-film is sandwiched between water drop and substrate. Accordingly, we presented a modified theoretical model of Young's equation considering a thin oil film beneath the water drop originating from surrounding viscous medium. On the other hand, the standard Young's equation do not translate to the underliquid systems on a glass substrate. Also, Owens-Wendt theory could not correctly predict the underliquid contact angles on glass. Therefore similar to PMMA, we hypothesize that a thin oil film is present beneath the water drop on glass substrate. However, the modified Young's equation with thin-film consideration agrees very well with the experimental values and thereby demonstrated the presence of a thin film between a drop and glass substrate originating from the surrounding viscous medium.

Acknowledgements

This thesis is the outcome of experiences and a lot of guidance from many people and I take this opportunity to thank everyone. First and foremost, I would like to express my sincere gratitude to my thesis supervisor, Dr. Sushanta Mitra, for offering such a great opportunity to join the Micro Nano Transport Laboratory (MNTL) at University of Waterloo. His guidance, encouragement and enthusiasm helped me in all the time of research and in completing my graduate studies.

I would like to thank my examining committee, Dr. Carolyn Ren and Dr. Boxin Zhao for their valuable time and suggestions.

I am grateful to the Natural Sciences and Engineering Research Council (NSERC) of Canada for the financial support through research grants. I am thankful to all the present and past members of MNTL, Dr. Naga Siva Kumar Gunda, Dr. Shyam Badu, Ayan Mazumdar and Sirshendu Misra. I would like to specially thank Dr. Naga Siva Kumar Gunda, post doctoral fellow at MNT Lab, for familiarizing me with all the experimental facilities and the guidance in completing my project. I would also like to thank Sirshendu Misra for the helpful discussions, the late nights we were working together before deadlines, and for all the fun we have had.

Finally, I would like to express my profound gratitude to my parents, Miku baa, Bhindew and Mrig for providing me with unfailing support and continuous encouragement throughout my stay far from home, through the process of researching and writing this thesis.

This accomplishment would not have been possible without them. Thank you.
Thanks for all your encouragement and much love to my little nephew Yash!

Dedicated to

Maa-Dita

&

Mrig

Table of Contents

List of Tables

List of Figures

Nomenclature

θ	contact angle
μ	viscosity
γ	surface tension
ρ	density
E	energy
S	spreading parameter
R	radius
P	pressure

Subscripts

D	drop
A	advancing
ow	oil/water
oa	oil/air
os	oil/solid
sa	solid/air
f, o	oil film
la	liquid/air
S	surrounding medium
R	receding
wo	water/oil
wa	water/air
ws	water/solid
sl	solid/liquid
f, w	water film

Superscripts

d	dispersive component
Y	Young's equation
p	polar component
$O-W$	Owens and Wendt

Abbreviations

PMMA	Poly (methyl methacrylate)
DBP	Dibutyl Phthalate
DI	De-Ionized
AFM	Atomic Force Microscopy
PTFE	Polytetrafluoroethylene
CA	Contact Angle
TCA	Theoretical Contact Angle
OCA	Observed Contact Angle
RICM	Reflection Interference Contrast Microscopy

Chapter 1

Introduction

1.1 Motivation

Wetting studies involve the complex molecular interaction of two fluids (liquid-gas or liquid-liquid) when it comes into contact with a surface. The characteristic parameter that dictates the wetting signature is the contact angle between the solid and liquid surfaces. [1–6]. As a result, significant efforts are made to decipher the apparent contact angle [2, 7, 8]. Thus, the keys to understand wetting phenomena lies at the intersection of different aspects of physics, chemistry, and engineering. Whether we apprehend the fact or not, we encounter wetting systems in our day to day life activities. Starting from how rain drops slides down the windows of our rooms, water flowing down the faucet to our kitchen sink or bath tub resulting in a stream of water, that rapidly breaks into separate drops, to our water-proof jackets that let the droplet roll-off easily and so on. Also, nature offers ample examples of wetting and non-wetting phenomena such as the formation of dew drops on grass tips, water repellent lotus leaf, contaminant oil drops on fish scales [1, 9, 10] and

ducks greasing their feathers to maintain them as water repellent [11]. Such interesting natural phenomena, creates a massive upsurge in efforts within the scientific community to explore the surface composition and understand how a liquid drop wets a surface to create liquid repellent surfaces, design functional interfacial materials and so on [12–14].

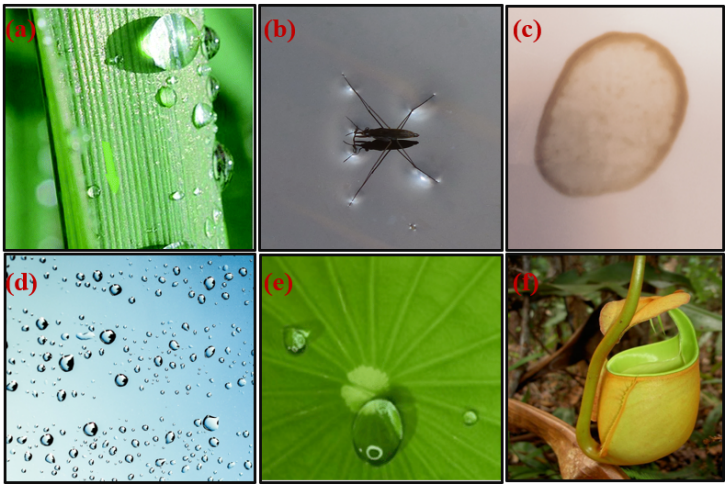

Figure 1.1: Various wetting surfaces.(a) Directional wetting of rice leaf (b) A water strider standing on water (c) A coffee stain formed upon evaporation of a coffee drop.
(d) Rain drops on window panes (e) Self cleaning lotus leaf (f) Slippery mouth of pitcher plant. Images are reproduced from Creative Commons.

Apart from these, due to the key role of wetting in diverse applications of paintings, printing inks, paper coatings, detergents etc. [15–17], wetting studies are thoroughly carried out for a variety of liquids and solid substrates. But limited studies are related to how the same wetting liquids and the substrates would behave when exposed to the viscous surrounding medium instead of an inviscid air medium. Only a handful of experimental [13, 18–22] and theoretical models [13, 23] report the investigation on liquid-liquid-solid

phase interaction. The present study intends to address some of the fundamental aspects concerned with underliquid wetting.

1.2 Organization of Thesis

This thesis is laid out based on a published work. It shows the underlying difference in wetting signature of a droplet in contact with a substrate placed in surrounding air medium to the wetting signature of the droplet on a substrate placed in surrounding viscous medium. Thereby, this thesis demonstrates and elucidates a new modified theoretical model that explains the anomalous wetting of two underliquid systems : oil (drop) in water medium and water (drop) in viscous oil medium.

The thesis consists of 5 chapters. Chapter 1 (the present chapter) delivers the introduction to the thesis and presents the basic motivation with the objectives of the thesis.

Following the introductory part is the Chapter 2 that summarizes the prior research on wetting phenomena. This review is focused more on the underliquid wetting.

Chapter 3 provides a brief description on the theory that forms the foundation of the underliquid wetting phenomenon illustrated thereafter in this thesis. First part of this chapter explicitly emphasizes on the determination of surface tension of liquids/solids and their components. In the next part of this chapter, we focus on the conventional wetting theories used for determination of contact angle in air and underliquid systems.

Chapter 4 describes the experimental details of underliquid wetting of two different systems namely, oil (drop) in water (surrounding medium) and water (drop) in oil (surrounding medium) with two different substrates viz., Poly (methyl methacrylate) PMMA

and glass. It illustrates the materials properties in detail along with the experimental procedures and the schematic representations of the setup.

Chapter 5 presents the results with discussion on the wetting study of underliquid systems. A distinctive anomaly when compared to the outcomes predicted by conventional wetting theories (as described in Chapter 3) has been noted and a hypothesis is proposed to explicate this difference. Later, the hypothesis is used to validate the thesis statement. With the proposed theory, we spot out the why the conventional wetting theories in air medium does not hold true for underliquid wetting systems.

Chapter 6 gives a summary of this thesis as well as briefly discuss on the scope and directions of the future work.

Chapter 2

Literature Review

Bartell and Osterhof [24] in 1927 first showed theoretically how the wetting of a liquid-liquid-solid interaction can be predicted depending on the contact angle values of each liquid for the same substrate kept in the air medium, by applying Young's equation [13, 19].

Seveno et al. [23] put forward a theoretical model for dynamic wetting of systems that comprises two immiscible liquids, where one liquid displaces another liquid from the substrate. This model was validated experimentally for oil (drop) in surrounding water medium as described by Goossens et al., [18] but no experimental data were provided for the inverse system, i.e., water (drop) in surrounding viscous medium.

van Dijke and Sorbie [25, 26] used the Bartell and Osterhof equation to quantify the wettability of a pore from oil-water contact angle, $\cos\theta_{ow}$. They adopted linear relationships of spreading and non-spreading oils to predict the angles in air medium i.e., oil drop in air, $\cos\theta_{oa}$ and water drop in air, $\cos\theta_{wa}$. They adopted these relations as functions of $\cos\theta_{ow}$ for strongly oil-wet pores ($\cos\theta_{ow}$=-1) and strongly water wet ($\cos\theta_{ow}$=1) pores. This was

carried out to see how they are related as functions of $\cos\theta_{ow}$ when it has arbitrary values between -1 and 1.

Grate et al. [27] reported the contact angle data for air-water and oil-water of modified silica surfaces with different silane reagents on silicone wafer materials. Here, they established correlation between the cosine of oil-water and water air contact angles with the experimental and van Dijke and Sorbie theory [25, 26].

Fetzer et al. [28, 29] demonstrated the spreading of a dodecane oil droplet on alkane thiol-coated gold surfaces kept in surrounding water medium whereby the ratio for the viscosities of drop to surrounding medium was fixed ($\mu_D/\mu_S \sim 1.5$). In addition, they correlated between the hydrophobicity of the surface with the contact line friction and found that the dynamic behavior of the liquid-liquid contact line is similar on two substrates with different hydrophobicities (thiol-coated gold surfaces and silane coated glass substrates).

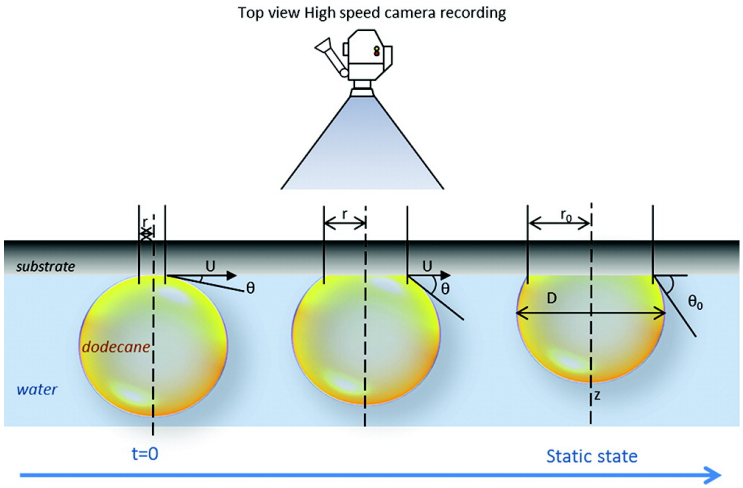

Figure 2.1: Schematic of a dodecane drop displacing water from the immersed solid surface. Reproduced from Ramiasa et al. [29] with permission from ACS Publications

Goossens et al. [18] correlated the wetting dynamics between liquid-liquid and liquid-air systems. They studied for series of oil droplets (dodecane, dibutyl phthalate (DBP), hexane, squalane and hexadecane) in air and in water medium on a hydrophobic grafted silicon substrate and tried to explain possible discrepancy of their results in comparison with the prediction based on Young's equation, as presented by Bartell and Osterhof [24]. They reported that the contact line may be pinned at heterogeneities when contact line velocity gets low. They mentioned that the Bartell Osterhof relation does not consider the hysteresis and thus should be used carefully used when compared to real systems that exhibit always a hysteresis.

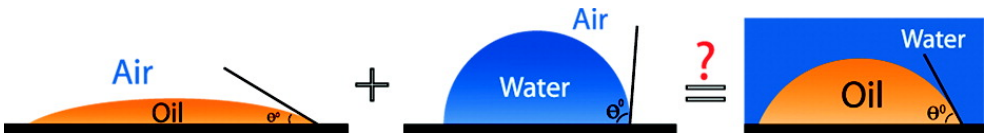

Figure 2.2: Schematic representation by Goosens et al. [18] to establish a link between the dynamics of wetting in liquidliquid and in liquidair systems. Image is reproduced with permission from ACS Publications

Jung and Bhushan [13] presented the theoretical model based on Young's equation for two fluid system to predict the oleophobic/phillic nature of the surfaces. To validate the model, they carried out investigation with water drop in air, oil drop in air and oil drop in water to study the wetting on flat and micropatterned surfaces. While their work clearly presents the nature of hydrophobic/phillic and oleophobic/phillic surfaces at various interfaces and found good agreement with the theoretical model, it does not compare the wetting characteristic for water drop in oil medium.

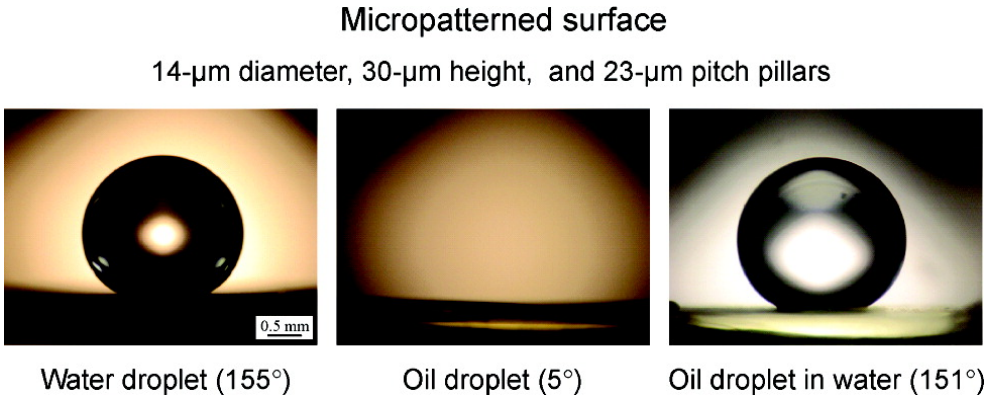

Figure 2.3: Optical images of droplets at three-different-phase interfaces on a micropatterned surface. Reproduced from Jung et al. [13] with permission from ACS Publications

Goswami and Bhagwat [30] carried out contact angle measurements for water drop in air and groundnut oil on under-water glass substrate, stainless steel, Teflon, nylon. They compared with the underwater contact angles with Young's equation but observed the discrepancy between the observed and theoretical comparison for underwater contact angles on glass, Teflon, and stainless steel. This difference is reported as the possible modification of surfaces when placed underwater. However, they got better agreement for stainless steel, polyamide and nylon surfaces with Girifalco, Goods, Fowkes approach. [31–33].

According to the theory proposed by Goods and Girifalco, surface free energy of some solids can be determined from the contact angle values of liquids on them. Fowkes [33] investigated mainly systems containing substance (solid or liquid) in which only the dispersion interactions appear. Owen and Wendt [34–37] continued the Fowkes formulation and considered both polar and dispersive components to find the surface free energy of a solid.

Understanding the wetting of drop on a substrate in the air medium is also contributed to study the spreading of the drop due to unbalanced interfacial tension driving it to its state of lowest energy. [38–43]

Recently, Mitra et al. [5] presented the early spreading of an oil droplet in an underwater substrate, where they observed the spreading process of laser oil and DBP on glass substrate submerged in a water medium. The viscosity ratios between the drop and the surrounding medium were 16 and 200. They inferred that spreading of sessile drops always begins in a viscous regime for a wide range of viscosity ratios of the drop and the surrounding medium. However, they do not consider the system for water drop spreading on a substrate kept in a viscous surrounding oil medium that yields very small ratios of the drop viscosity to the surrounding liquid viscosity ($\mu_D/\mu_S \ll 1$). Thus, it is seen that even though there have been sincere attempts to examine the wetting of the two-liquid system, yet there is a dearth of explanations to comprehensively understand the wetting of water (drop) in surrounding viscous oil medium.

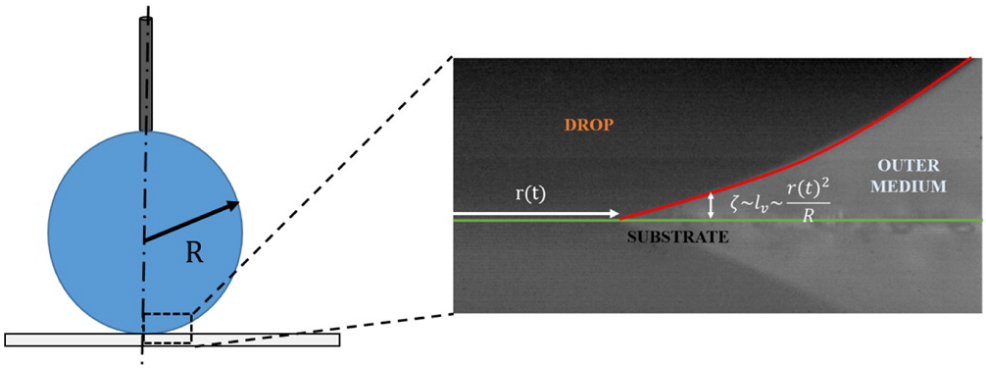

Figure 2.4: Initial stage of a liquid drop (of radius R) spreading on a substrate kept in a surrounding medium. Reproduced from Mitra and Mitra [5] with permission from ACS Publications

More recently, Ozkan and Erbil [19] characterized the wetting phenomena for systems which involve both oil (drop) in water and water (drop) in oil medium. They introduced the 'complementary hysteresis model' which relates the interfacial tensions of oil-water with the complementary angles of water (drop)-oil and oil (drop)-water. According to the model, if the surface energy of substrate in air is available, it is possible to predict the behavior of a substrate when immersed into oil or water by using the 'complementary hysteresis' approach. They observed that 'complementary hysteresis' of a substrate is directly proportional to the total surface energy of the solid. Their study only infers on the relation between substrate surface energy determined in air and the equilibrium contact angles for various substrates observed in oil-water systems. It doesn't explore to describe the wetting behavior for a water drop kept submerged under oil medium. Hence, even though wetting characteristics have been studied for two liquid system, there is an inadequate understanding of wetting of water (drop) on a substrate in surrounding viscous oil medium.

Chapter 3

Theory

The fundamental property of liquids as a result of which we witness innumerable everyday instances, starting from early morning dew drops, pin floating on water, not sticking of mercury used in the thermometer and so on is known as the surface tension. When two different phases (air/liquid, liquid/liquid, air/solid or liquid/solid) are in contact with each other the molecules at the interface experience an imbalance of forces. Liquid molecules inside the bulk medium are in an energetically favourable state as they are pulled equally in all directions by their neighbouring molecules of same species. Hence, they have a net resultant force equivalent to zero. However, liquid molecules at the interface are attracted only to the other surface molecules and to the molecules below the surface. This enhancement in the attractive forces at the interface is called surface tension.

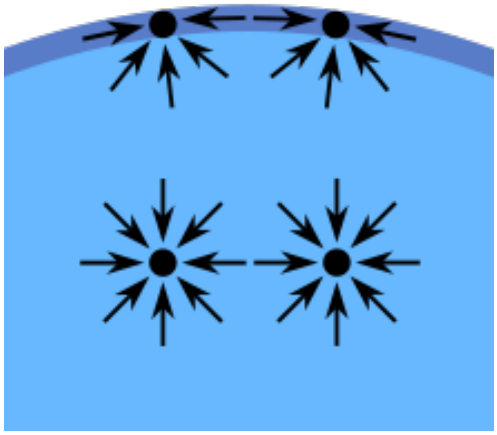

Figure 3.1: Representation of the forces on molecules of a liquid

However, if the surface considered is the interface of two immiscible liquids, the measurement is referred to as interfacial tension. The surface tension/interfacial tension is denoted phase by γ. Its units are measured as energy per surface, [J/m^2] or force per wetted length, [N/m].

3.1 Determination of oil surface tension components

The interaction between the atoms and molecules that causes the surface energy/tension of a substance can be described by two different types i.e., dispersive and polar components. Interactions caused by temporary fluctuations of the charge distribution in the atoms/molecules are called dispersive interactions (van der Waals interactions). Polar interactions comprise Coulomb interactions between permanent dipoles and between permanent and induced dipoles (e.g. hydrogen bonds). The surface tension of oils is usually

expressed as the sum of the dispersive and polar components. Therefore, it can be expressed as

$$\gamma_{oa}^{p} + \gamma_{oa}^{d} = \gamma_{oa} \tag{3.1}$$

where, γ is the surface tension and superscripts "*d*" and "*p*"are related to the dispersive and the polar components of the surface tension of oil. The dispersive and polar components of the oils can be determined using the relation for oil/water interfacial tension [31, 32].

$$\gamma_{ow} = \gamma_{oa} + \gamma_{wa} - 2(\gamma_{oa}^{d}\gamma_{wa}^{d})^{1/2} - 2(\gamma_{oa}^{p}\gamma_{wa}^{p})^{1/2} \tag{3.2}$$

where, subscripts "*oa*", "*wa*" and "*ow*" refer to oil/air, water/air and oil/water interfaces, respectively and superscripts d and p are related to the dispersive and the polar components of surface tension. Now,γ_{oa}^{p} can be expressed in terms of γ_{oa}^{d} from Eq. 3.1. Therefore we can rewrite the Eq. 3.2 as

$$\gamma_{ow} = \gamma_{oa} + \gamma_{wa} - 2(\gamma_{oa}^{d}\gamma_{wa}^{d})^{1/2} - 2((\gamma_{oa} - \gamma_{oa}^{d})\gamma_{wa}^{p})^{1/2} \tag{3.3}$$

We use the polar and dispersive components of water from the literature [35] i.e., γ_{wa}^{p} = 46.4 mN/m and γ_{wa}^{d}= 26.4 mN/m.

Substituting the surface tension of oil and water, interfacial tension of oil/water, and polar and dispersive components of water in Eqs. 3.3 and 3.1, one can determine the dispersive and polar components of oil.

3.1.1 Wetting in air

Typically, for the interaction of a liquid (drop) on a solid (substrate) in air (surrounding medium), we have a contact line where the three phases meet. The shape of a drop on a

smooth surface depends on the force balance. According to De-Gennes [1], the spreading parameter, S is defined as

$$S = \gamma_{sa} - (\gamma_{sl} + \gamma_{la})$$

which determines the surface energy per unit area of the substrate when wet and dry.

If $S > 0$, the liquid phase tend to spread indefinitely to minimize its surface area.

If $S < 0$, the liquid will only wet a finite area and tend to form a spherical cap on the substrate with an equilibrium contact angle θ. At an equilibrium state of a droplet, by force balance we can write

$$\cos\theta_{oa} = \frac{(\gamma_{sa} - \gamma_{sl})}{\gamma_{la}} \tag{3.4}$$

where γ represents the surface tension (or surface free energy) and the subscripts "sl", "la" and "sa" refer to solid/liquid, liquid/air, and solid/air interfaces, respectively and θ_{oa} is the equilibrium contact angle of oil drop on a substrate in air medium.

This equation is known as the Young's equation at equilibrium. The contact angle is determined by the sessile drop method by measuring the angle between the tangent along solid-liquid interface and liquid-air interface as shown in Fig. 3.2. A contact angle of 0° corresponds to complete wetting and 180° corresponds to non-wetting.

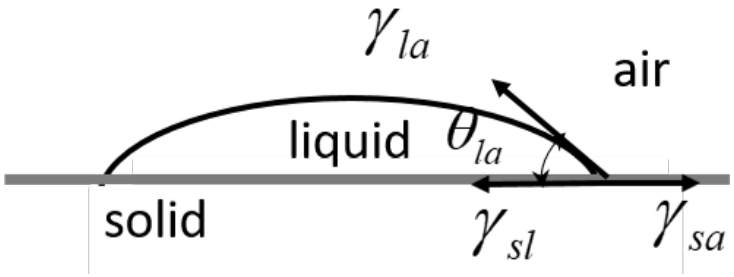

Figure 3.2: Schematic representation (not to scale) of liquid (drop) in air

3.1.2 Calculation of surface energy of solid

In order to calculate the surface energy of a solid substrate, two test liquids with known contact angles on the solid substrate and known surface tensions including their dispersive and polar components are selected. As discussed above, Young's equation for a liquid droplet on a given substrate in air medium can be arranged as

$$\gamma_{sl} + \gamma_{la} cos\theta_{la} = \gamma_{sa}$$

The combining rule proposed by Owens, Wendt, Rabel and Kaelble (OWRK) model is indicated below [34]

$$\gamma_{sl} = \gamma_{sa} + \gamma_{la} - 2(\gamma_{sa}^{d}\gamma_{la}^{d})^{1/2} - 2(\gamma_{sa}^{p}\gamma_{la}^{p})^{1/2} \tag{3.5}$$

Substituting γ_{sl} from Young's equation to Eq. 3.5 , one can rearrange the Eq. 3.5 as expressed below

$$(\gamma_{sa}^{d}\gamma_{oa}^{d})^{1/2} + (\gamma_{sa}^{p}\gamma_{oa}^{p})^{1/2} = \frac{1}{2}[\gamma_{sa} + \gamma_{la} - (\gamma_{sa} - \gamma_{la} cos\theta_{la})] \tag{3.6}$$

$$(\gamma_{sa}^{d}\gamma_{la}^{d})^{1/2} + (\gamma_{sa}^{p}\gamma_{la}^{p})^{1/2} = \frac{1}{2}[\gamma_{la}(1 + cos\theta_{la})] \tag{3.7}$$

Dividing both the sides of the above equation by γ_{la}^{d}, one can arrive as the following equation

$$(\gamma_{sa}^{d})^{1/2} + (\gamma_{sa}^{p})^{1/2}(\frac{\gamma_{la}^{p}}{\gamma_{la}^{d}})^{1/2} = \frac{1}{2}[\frac{\gamma_{la}(1 + cos\theta_{la})}{(\gamma_{la}^{d})^{1/2}}] \tag{3.8}$$

Hence, the above equation can be expressed in the linear form,

$$y = mx + c \tag{3.9}$$

where,

$$y = \frac{1}{2}[\frac{\gamma_{la}(1 + cos\theta_{la})}{(\gamma_{la}^{d})^{1/2}}]$$

$$m = (\gamma_{sa}^{p})^{1/2}$$
$$x = (\frac{\gamma_{la}^{p}}{\gamma_{la}^{d}})^{1/2}$$
$$c = (\gamma_{sa}^{d})^{1/2}$$

The slope of the graph gives the polar component and the vertical intercept gives the dispersive component of the solid surface free energy.

3.1.3 Calculation of solid/liquid interfacial tension

For different liquids and solids combination, the interfacial tension of solid/liquid can be calculated [31–35].

$$\gamma_{so} = \gamma_{sa} + \gamma_{oa} - 2(\gamma_{sa}^{d}\gamma_{oa}^{d})^{1/2} - 2(\gamma_{sa}^{p}\gamma_{oa}^{p})^{1/2} \tag{3.10}$$

$$\gamma_{sw} = \gamma_{sa} + \gamma_{wa} - 2(\gamma_{sa}^{d}\gamma_{wa}^{d})^{1/2} - 2(\gamma_{sa}^{p}\gamma_{wa}^{p})^{1/2} \tag{3.11}$$

where subscripts "sa" refer to solid/air interface and superscripts "d" and "p" are related to the dispersive and the polar components of surface tension. Substituting the surface tension of oil, water and solid as well as dispersive and polar components of oil, water and solid, one can determine the solid/oil and solid/water interfacial tension.

3.1.4 Wetting in underliquid systems

In the present work, we investigated the wetting of oil (drop) in water medium and water (drop) in viscous oil medium on poly(methyl methacrylate) (PMMA) and glass substrates. Also, of interest here is to compare the two underliquid systems and check whether these two fluid systems satisfy the existing wetting theories.

3.1.4.1 Water (drop) in oil (surrounding medium): Bartell-Osterhof equation

In this section, the theoretical determination of contact angle calculation for water (drop) in oil medium is discussed using Young's equation.

As discussed above the Young's equation for a water droplet on a given substrate in air medium can be written as

$$\gamma_{sw} + \gamma_{wa} cos\theta_{wa} = \gamma_{sa} \tag{3.12}$$

where subscript "sw" refer to solid/water interface and θ_{wa} is the equilibrium contact angle of water drop on a substrate in air medium.

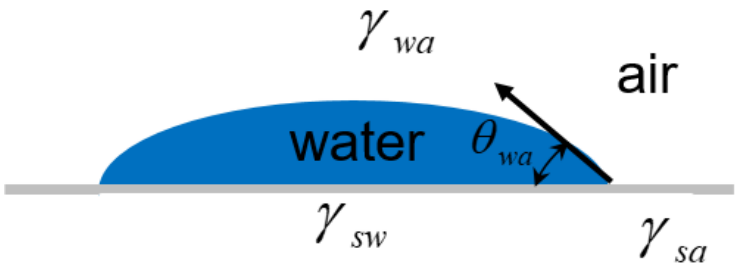

Figure 3.3: Schematic representation (not to scale) of water (drop) in air

Young's equation for oil drop on a given substrate in air medium can be written as

$$\gamma_{so} + \gamma_{oa} cos\theta_{oa} = \gamma_{sa} \tag{3.13}$$

where the subscript "so" refers to solid/oil interface and θ_{oa} is the equilibrium contact angle of oil drop on a substrate in air medium.

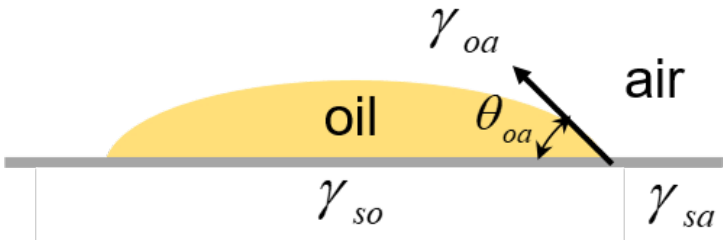

Figure 3.4: Schematic representation (not to scale) of oil (drop) in air

Also, Young's equation for water droplet on a given substrate in oil medium (Fig. 3.5) can be written as

$$\gamma_{sw} + \gamma_{wo} cos\theta_{wo} = \gamma_{so} \tag{3.14}$$

where the subscript "wo" refers to water/oil interface and θ_{wo} is the equilibrium contact angle of water drop in oil medium. Therefore substituting Eq. 3.12 and Eq. 3.13 in Eq. 3.14, one can arrive at the simplified equation to express the contact angle for water (drop) in oil, $\cos\theta_{wo}$

$$cos\theta_{wo} = \frac{(\gamma_{wa} cos\theta_{wa} - \gamma_{oa} cos\theta_{oa})}{\gamma_{wo}} \tag{3.15}$$

This equation is also known as Bartell-Osterhof equation [24].

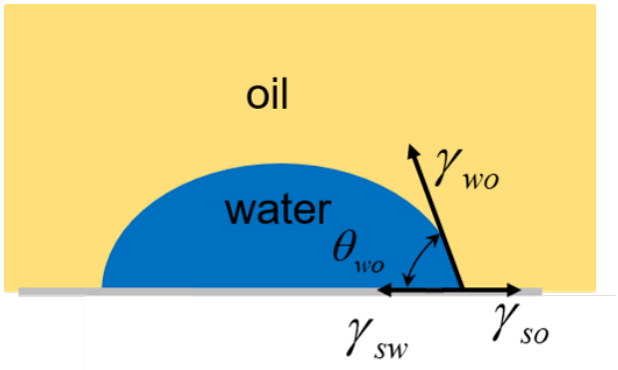

Figure 3.5: Schematic representation of water(drop) in oil medium

3.1.4.2 Water (drop) in oil (surrounding medium): Owens and Wendt theory

In this section, the theoretical determination of contact angle calculation for water (drop) in oil medium is discussed using the Owens and Wendt theory. Owens and Wendt proposed that the surface energy of a solid is comprised of two components i.e., a dispersive component and a polar component. The OwensWendt theory (also known as the Kaelble-OwensWendt method) involves the determination of components of dispersion and polar surface free energy. This is based on the Bethelot hypothesis that claims that molecular interaction of two substances, present on the surface layer, are interpreted as the geometric mean of the disperse and the polar component of the surface tension. So, they continued the Fowkes [33] formulation (which investigated mainly systems with dispersion interactions only) to estimate the interfacial energy. Hence, according to Owens and Wendt theory, one can estimate the solid/ liquid interfacial energies and thereby we used it to predict the underliquid contact angles. Therefore, substituting γ_{so} from Eq. 3.10 and γ_{sw} from Eq. 3.11 in Eq. 3.14 for water droplet on a given substrate in oil medium (Fig. 3.5), the contact angle for water (drop) in oil, $cos\theta_{wo}$ with Owens and Wendt theory, can be

expressed as

$$\cos\theta_{wo}^{O-W} = \frac{(\gamma_{oa} - 2(\gamma_{sa}^{d}\gamma_{oa}^{d})^{1/2} - 2\gamma_{sa}^{p}\gamma_{oa}^{p})^{1/2} - \gamma_{wa} + 2(\gamma_{sa}^{d}\gamma_{wa}^{d})^{1/2} + 2(\gamma_{sa}^{p}\gamma_{wa}^{p})^{1/2})}{\gamma_{ow}} \quad (3.16)$$

where, the subscripts "sa" refer to solid/air interface and superscripts "p" and "d" are respectively the polar components and dispersive components of surface tension.

3.1.4.3 Oil (drop) in water (surrounding medium) : Bartell-Osterhof equation

Young's equation for an oil drop on a given substrate in water medium (Fig. 3.6) can be written as

$$\gamma_{so} + \gamma_{ow} cos\theta_{ow} = \gamma_{sw} \quad (3.17)$$

where θ_{ow} is the equilibrium contact angle of oil drop on a substrate in water medium.

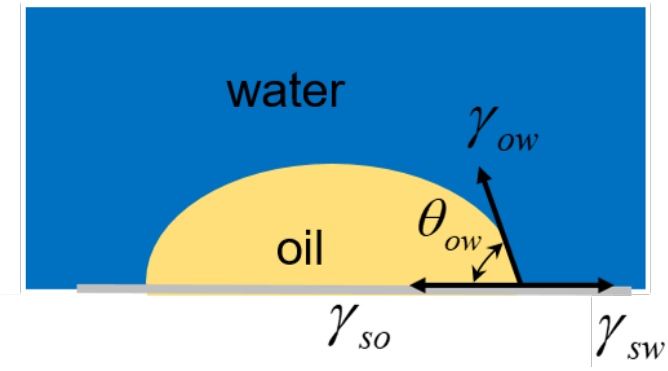

Figure 3.6: Schematic representation of oil (drop) in water (surrounding medium).

Therefore substituting Eq. 3.12 and Eq. 3.13 in Eq. 3.17, one can arrive at the simplified equation to express the contact angle for oil (drop) in water, $cos\theta_{ow}$

$$cos\theta_{ow} = \frac{(\gamma_{oa} cos\theta_{oa} - \gamma_{wa} cos\theta_{wa})}{\gamma_{ow}} \quad (3.18)$$

3.1.4.4 Oil (drop) in water (surrounding medium) : Owens and Wendt theory

In this section, the theoretical determination of contact angle calculation for oil (drop) in water medium is discussed using the Owens and Wendt theory. Therefore, we substitute γ_{so} from Eq. 3.10 and γ_{sw} from Eq. 3.11 in Eq. 3.17 for oil drop on a given substrate in water medium (Fig. 3.6) to express the contact angle for oil (drop) in water, $cos\theta_{ow}$ with Owens and Wendt theory and it is expressed as

$$\cos\theta_{wo}^{O-W} = \frac{\gamma_{wa} - 2(\gamma_{sa}^{d}\gamma_{wa}^{d})^{1/2} - 2(\gamma_{sa}^{p}\gamma_{wa}^{p})^{1/2}) - \gamma_{oa} + 2(\gamma_{sa}^{d}\gamma_{oa}^{d})^{1/2} + 2\gamma_{sa}^{p}\gamma_{oa}^{p})^{1/2}}{\gamma_{ow}} \quad (3.19)$$

where, the subscripts "sa" refer to solid/air interface and superscripts "p" and "d" are respectively the polar components and dispersive components of surface tension.

Chapter 4

Experimental Details

The aim of the experiments in this thesis is to provide a basic understanding of wetting of underliquid systems. As illustrated below, the experimental details includes the materials used, experimental setup and experimental procedures which consists of cleaning procedures, roughness measurements of substrates, measurements of contact angles.

4.1 Materials

The working liquids used were de-ionized (DI) water (MiliQ, 18.2 MΩ.cm, MilliPore Sigma, Ontario, Canada), laser oil (Cargille Laboratories Inc., Cedar Grove, NJ, USA), dibutyl phthalate (DBP), two different silicone oils, labeled as silicone oil-1 and silicone oil-2 with viscosities 48.1 mPa-s and 484.5 mPa-s, respectively (Sigma-Aldrich, Canada). All the oils and DI water (ρ = 1000 kg/m^3, μ = 1 mPa/s γ_{wa} = 72 mN/m, γ^p_{wa} = 46.4 mN/m, γ^d_{wa} = 26.4 mN/m) were used without any further treatment. The properties of the oils are provided in Table 4.1. Here the subscripts "o", "w", and "a" refer to oil, water, and air

phases, respectively.

Table 4.1: Properties of the oils used in the present study

Properties	**Symbols**	**DBP**	**Silicone oil-1**	**Laser oil**	**Silicone oil-2**
Density, (kg/m^3)	ρ	1043	963	1069	969
Viscosity, (mPa/s)	μ	16	48.1	130.4	484.5
Surface Tension,(mN/m)	γ_{oa}	32.7	20	24.5	20.9
Polar component, (mN/m)	γ_o^p	4.09	0.05	0.62	0
Dispersive component, (mN/m)	γ_o^d	4.09	0.05	0.62	0
Interfacial tension, (mN/m)	γ_{ow}	22.2	43.3	35.6	49.9
PMMA-liquid interfacial tension, (mN/m)	γ_{so}	0.038	3.79	1.50	4.46
Glass-liquid interfacial tension, (mN/m)	γ_{so}	20.79	37.82	31.27	40.69

The surface tension of oil (γ_{oa}) and oil-water (γ_{ow}) interfacial tension values, were measured with OCA20 Data Physics optical contact angle device (Data Physics Instruments, Germany) and compared with the literature. The surface tension of solids (γ_{sa}) was measured with Owens, Wendt, Rabel, and Kaelble (OWRK) method and SCA21 software (Data Physics Instruments, Germany). Furthermore polar and dispersive components of

the oils and solid-liquid interfacial tension were calculated and presented in Table 4.1 [20, 44] (details on calculations of polar and dispersive components of oils and solids are already discussed in Chapter 3). Microscopic glass slides of dimensions 75 mm×25 mm×1 mm (Fisher scientific, Canada) and PMMA sheets of 150 mm×150 mm×1 mm (Plaskolite Inc., USA) were diced into 25 mm×25 mm square pieces and used as the substrate material. A distortion-free glass cuvette (SC-01, Krüss, Hamburg, Germany) of inner dimension 30 mm×30 mm×25 mm with 2.5 mm thickness was used to hold the surrounding liquid medium for all experiments. The solid substrates used are Poly (methyl methacrylate) (PMMA) and glass. The properties of the solids are provided in Table 4.2.

Table 4.2: Properties of the solids used in the present study

Solids	Surface tension γ_{sa} (mN/m)	Polar component γ_{sa}^{p} (mN/m)	Dispersive component γ_{sa}^{d} (mN/m)
PMMA	30.68	4.13	26.55
Glass	55.68	40.28	15.20

4.1.1 Cleaning of substrates

To start with any experiment, the glass substrates were thoroughly cleaned in ethanol, subjected to sonication in an ultrasonic bath (Branson M5800, Emerson Electric Canada Ltd, Canada) for 10 minutes and then cleaned with DI water. After that, the glass substrates were dried under nitrogen before any measurements were carried out. Similarly, the PMMA substrates were cleaned with hexane to get rid of any debris present on the surface and rinsed with DI water for about 5 min. The PMMA substrates were also dried with nitrogen gas.

4.1.2 Roughness measurement of substrates

4.1.2.1 Atomic force microscopy

Atomic force microscopy (AFM) provides a unique facility to measure local properties, such as height, friction, magnetism with a cantilever that has a very high resolution probe to scan over a sample surface. To record the images, the probe is scanned over a small sample surface to measure the local property simultaneously. Here, for the detection of cantilever deflections towards or away from the surface a laser beam is used. Changes in the direction of the reflected light beams is used to detect cantilever deflections. A position-sensitive photo diode (PSPD) is used to track these changes. Thus, if an AFM tip passes over a raised surface feature, the resulting cantilever deflection (and the subsequent change in direction of reflected beam) is recorded by the PSPD. A feedback loop is used to control the height of the tip above the surface and thus constant laser position is maintained. AFM can generate an accurate topographic map of the surface features.

4.1.2.2 Surface profilometer

A surface profilometer is a measuring instrument that is used to quantify a surface's profile, in terms of its roughness, waviness, and other finish parameters. Stylus-based, surface profilometers are used to measure surface texture by dragging a sharp, tool across the sample surface. The tip movements are recorded to calculate the height variations then used to form a texture profile. Roughness and waviness are also calculated from the surface profile data.

We used atomic force microscopy (Dimension 3100, Digital Instruments, Indianapolis,

USA) and surface profilometer (P-6 Surface Profiler System, KLA Tecncor, California, USA) to check the roughness of the PMMA and glass substrates used in the present work. For AFM, we scanned the area of 15μm $\times$ 15μm and observed a root mean square (rms) roughness of 34.961 nm and 2.716 nm for PMMA and glass, respectively. For surface profilometer, we considered a larger scan length of 512μm and observed a roughness of 31.38 nm and 2.58 nm for PMMA and glass, respectively.

4.1.3 Measurement of static and dynamic contact angles

Measurement of sessile drop static contact angles and the dynamic contact angles (advancing and receding) were carried out for different liquids in air medium, water (drop) in oil medium and oil (drop) in water medium on PMMA and glass substrates. A customized contact angle measurement instrument located at the Micro & Nanoscale Transport laboratory in Waterloo Institute for Nanotechnology was used to conduct the experiments. For each image of the drop, a tangent method [45, 46] was applied to obtain the contact angle value from the slope observed at the three-phase contact line. The contact angle values were extracted with Holmarc contact angle software (Holmarc Opto-Mechatronics Pvt Ltd., Kochi, Kerela, India). The contact angles illustrated here are the average values of five (5) measurements on different samples.

A liquid drop of $3\mu L$ volume (the drop volume is kept small so that the radius of drop is considerably smaller than its corresponding capillary length) was formed quasi-statically at the tip of a stainless steel needle and deposited on the substrates (i.e., PMMA or glass) to measure the contact angle in air medium. For dynamic contact angle measurement, the drop volume was increased from 1 μL to 10 μL and decreased from 10 μL to 1 μL to measure the advancing (θ_A) and receding (θ_R) contact angles, respectively.

As presented in Table 4.1, the working liquids have a wide range of density (963 - 1069 kg/ m^3). As mentioned earlier, the two systems investigated here are water (drop) in oil medium and oil (drop) in water medium on PMMA and glass substrates. Therefore, in order to measure the contact angle (static and dynamic) of the denser liquid droplet in lighter surrounding medium, the substrate was kept at the bottom of a distortion-free glass cuvette and the drop was deposited with a stainless steel needle having an inner diameter of 1.1 mm, as shown in Figs. 4.1(a) and 1(b). For the measurement of the contact angle (static and dynamic) of the lighter liquid droplet in denser surrounding medium at static equilibrium, the substrate was fixed to the side wall of the distortion-free glass cuvette at the air-liquid interface with a magnetic clip and a J-needle (PTFE, Krüss, Hamburg, Germany) was used to generate the inverted droplet, as shown in Figs. 4.1(c) and 1(d).

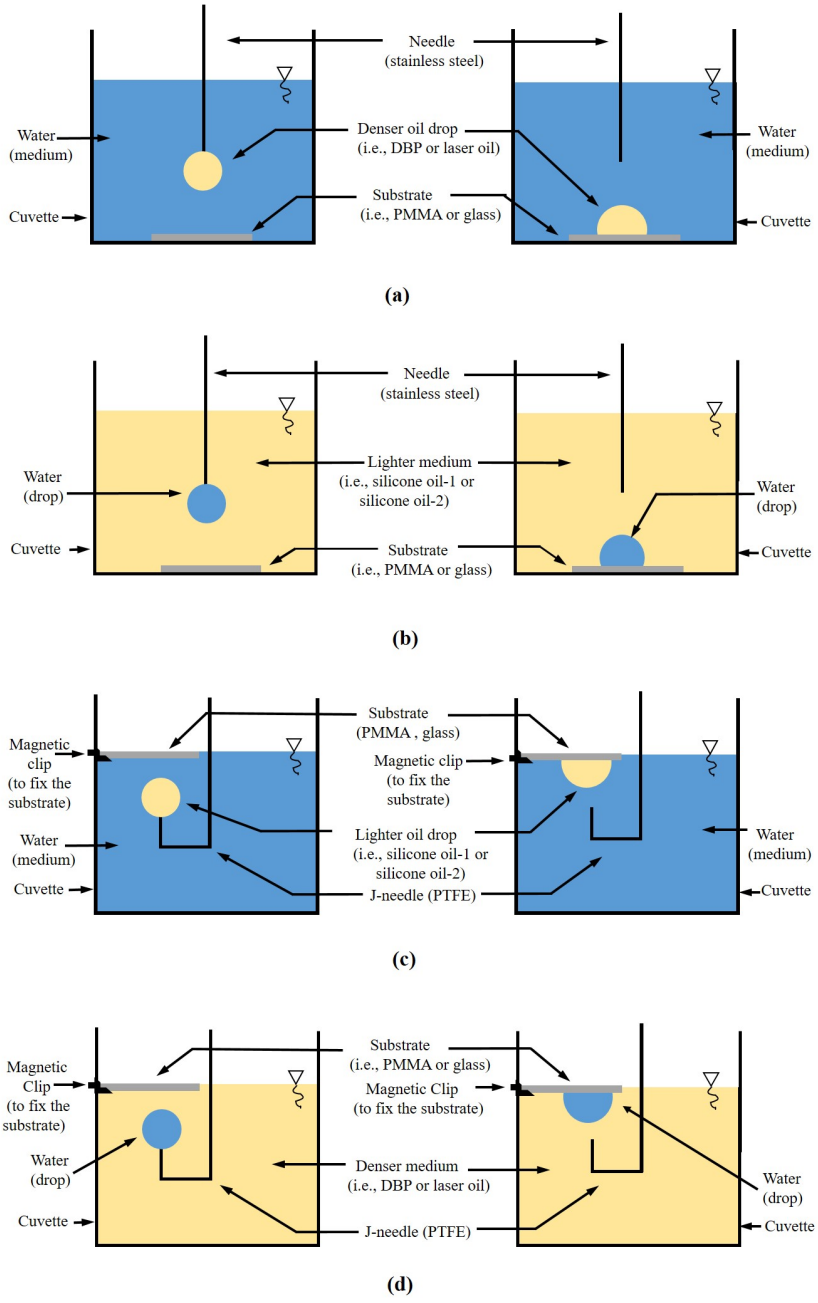

Figure 4.1: Schematic of drop deposition (before and after) (a) oil drop (denser) in water medium (b) water drop in lighter oil medium (c) oil drop (lighter) in water medium (d) water drop in denser oil medium.

Chapter 5

Results and Discussion [1]

5.1 Liquid drops in air medium

The static and dynamic contact angles of the working liquids (water and oils) in air medium on both PMMA and glass are presented in Table 5.1. Water (drop) on PMMA substrate in air medium was found to have a static contact angle of 76°±2° with advancing (θ_A) / receding contact angles (θ_R) of 84°±2°/70°±2°. Whereas, on a glass substrate the static contact angle of water was found to be 14°±2° and θ_A/θ_R of 22°±2.3°/7°±2°. The optical images of water (drop) on both PMMA and glass are presented in Figs. 5.1(a) and 5.1(b), respectively. This clearly shows that PMMA is hydrophobic in nature while glass is hydrophilic. Similarly, static contact angle of DBP on PMMA and glass is 9°±2° and 16°±2°, respectively. Figs. 5.1(c) and 5.1(d) shows the optical images for DBP (drop) in air medium on PMMA and glass, respectively. Laser oil has a static contact angle of 10°±4.5° on PMMA and 11°±3° on glass. On PMMA, silicone oil-1 and silicone oil-2 have a static contact angle of 10.7°±3° and 11°±2°, respectively. Whereas on glass, the

[1] Reproduced from Trinavee, K.; Gunda, N. S. K.; Mitra, S. K. *Langmuir* **2018**, 34, 11695-11705.

respective static contact angles are 10°±2.5° and 14°±2°. The advancing and receding contact angles, θ_A/ θ_R for different oils on both PMMA and glass are presented in Table 5.1. Therefore, we observe that oil (drop) in air medium has slightly higher contact angle values on glass substrate compared to PMMA.

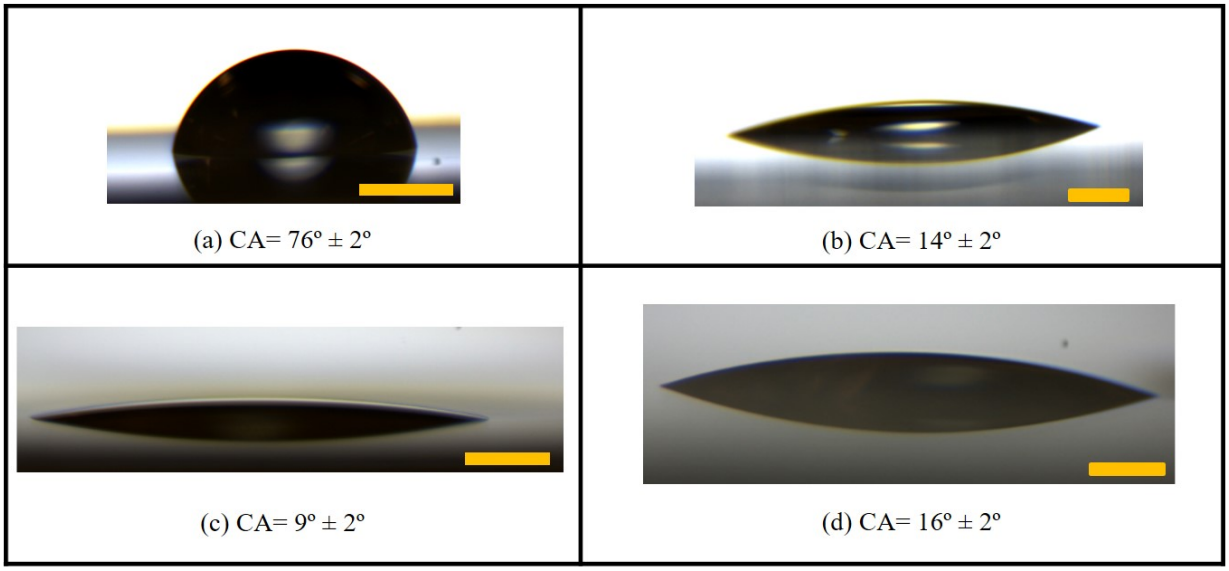

Figure 5.1: Optical images of (a) water (drop) on PMMA (b) water (drop) on glass (c) DBP drop on PMMA (d) DBP on glass in air medium. The scale bar represents 1 mm.

Table 5.1: Static and dynamic contact angles (CA) of liquid drops in surrounding air medium on PMMA and glass substrates

Liquids	on PMMA Static CA	on PMMA θ_A/θ_R	on Glass Static CA	on Glass θ_A/θ_R
Water	76°±2°	84°±2°/70°±2°	14°±2	22°±2.3°/7°±2°
DBP	9°±2°	19°±2°/7°±2.5°	16°±2°	27°±2°/10°±2°
Laser oil	10°±4.5°	19°±4.5°/8°±4.5°	11°±3°	21°±2.5°/7°±3
Silicone oil-1	10.7°±3°	20°±3°/8°±3°	10°±2.5°	22°±2°/6°±2.5°
Silicone oil-2	11°±2°	20°±2° /9°±2°	14°±2°	23°±2°/6°±2°

5.1.1 Water drop in oil medium

In Table 5.2, we have illustrated the wetting of water (drop) in oil medium on PMMA and glass with the static and dynamic contact angle measurements. The static contact angles of water (drop) in DBP (as shown in Fig. 5.2(a)) and laser oil on a PMMA substrate are 146°±3° and 136°±4°, respectively. Also, we observed advancing/receding contact angles, θ_A/θ_R of 150°±2°/136°±2° and 157°±2°/120°±3.5° with DBP and laser oil as surrounding media, respectively. Thus, we see that water (drop) has slightly higher contact angle in DBP (medium) than laser oil (medium) on PMMA. Similarly, water (drop) in silicone oil-1 (shown in Fig. 5.2(b)) and silicone oil-2 on the submerged PMMA substrate has static contact angles of 137°±4° and 139°±4.3°, respectively. The observed advancing/receding contact angle values are presented in Table 5.2. In literature [21], it is reported that for water (drop) on a thin lubricant film of silicone oil (10mPa-s, different from the one used here), the equilibrium contact angle is 120°. Though the two systems are different, however this provides some ballpark value of contact angle for oil drop on PMMA substrate

submerged inside a viscous silicone oil.

Table 5.2: Static and dynamic contact angles of water (drop) in oil (surrounding medium) on PMMA and glass substrates

Liquids	on PMMA Static CA	on PMMA θ_A/θ_R	on Glass Static CA	on Glass θ_A/θ_R
DBP	146°±3°	150°±2°/136°±2°	42°±2°	46°±3°/35°±2°
Laser oil	136°±4°	157°±2°/120±3.5°	143°±2°	156°±2°/135°±3°
Silicone oil-1	137°±4°	142°±2°/130°±3°	96°±2°	110°±2°/80°±2.1°
Silicone oil-2	139°±4.3°	144°±2.5°/132°±2°	113°±2.5°	122°±3.3°/90±2°

On the glass substrate, the static contact angle of water (drop) in DBP (as shown in Fig. 5.2(c)) is 42°±2° and we observed θ_A/θ_R of 46°±3°/35°±2°. This shows that water (drop) has a very low contact angle on glass substrate in DBP (surrounding oil medium) that has a very low viscosity of 16 mPa-s and smaller water-oil interfacial tension of 22.2 mN/m. However, for glass substrate in laser oil (130.4 mPa-s), with higher oil-water interfacial tension compared to DBP, we observed a higher static contact angle of 143°±2°. Water (drop) on glass substrate in silicone oil-1 (shown in Fig. 5.2(d)) and silicone oil-2 have static contact angles of 96°±2° and 113°±2.5°, respectively. The advancing/receding contact angles, θ_A/θ_R for laser oil, silicone oil-1 and silicone oil-2 are provided in Table 5.2. Therefore, we found that contact angle of water (drop) in silicone oil-1 (48.1 mPa-s) and silicone oil-2 (484.5 mPa-s) are nearly the same because the individual surface tension and oil-water interfacial tension for both the oils are nearly the same. However, the small difference in the contact angle values is due to the difference in their viscosities.

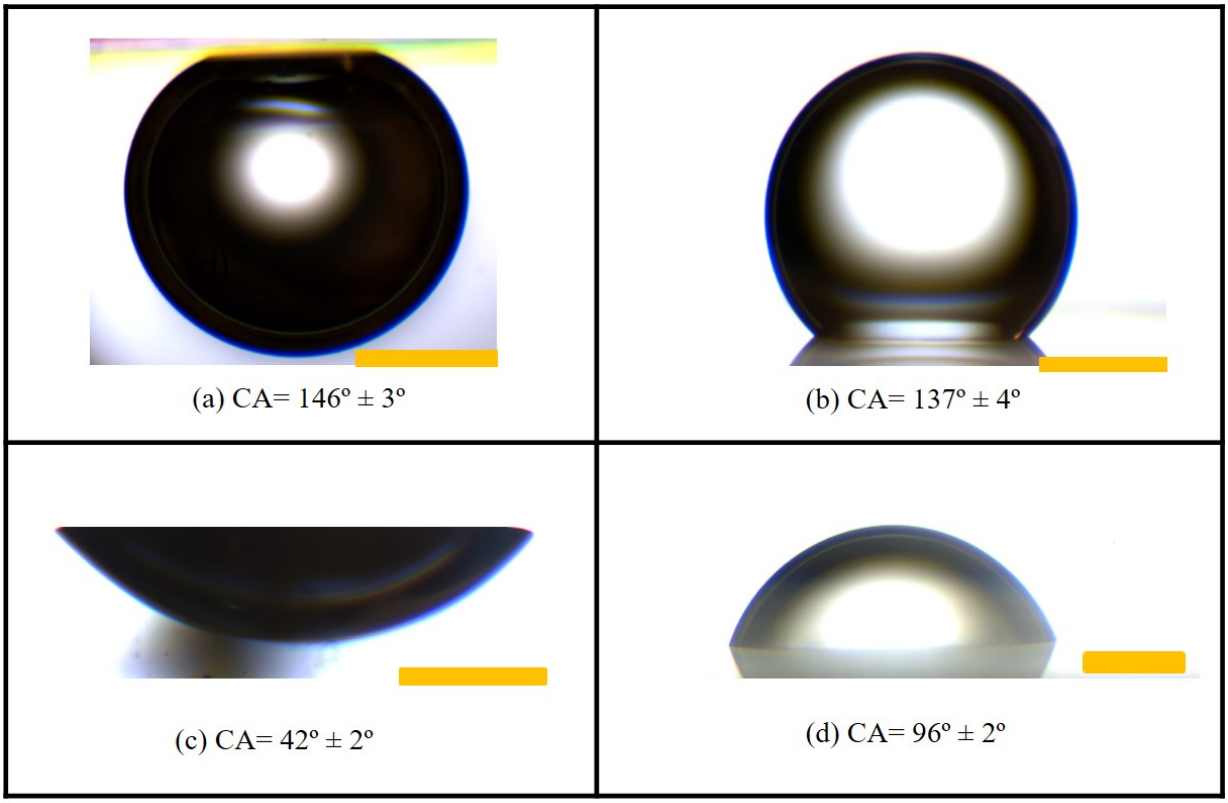

Figure 5.2: Optical images of water (drop) in different oil medium (a) water (drop) in DBP on PMMA (b) water (drop) in silicone oil-1 on PMMA (c) water (drop) in DBP on glass (d) water (drop) in silicone oil-1 on glass. The scale bar represents 1 mm.

5.1.2 Oil drop in water medium

The wetting behavior of oil (drop) in water (surrounding medium) on PMMA and glass substrate is illustrated in Table 5.3. The static contact angle of DBP (drop) on the underwater PMMA substrate is 53°±2° (as shown in Fig. 5.3(a)) and exhibited advancing/receding contact angles, θ_A/θ_R of 63°±2°/48°±3°. Similarly, we observed the static contact angle of laser oil (drop) on the underwater PMMA substrate is 76°±4.5° and θ_A/θ_R

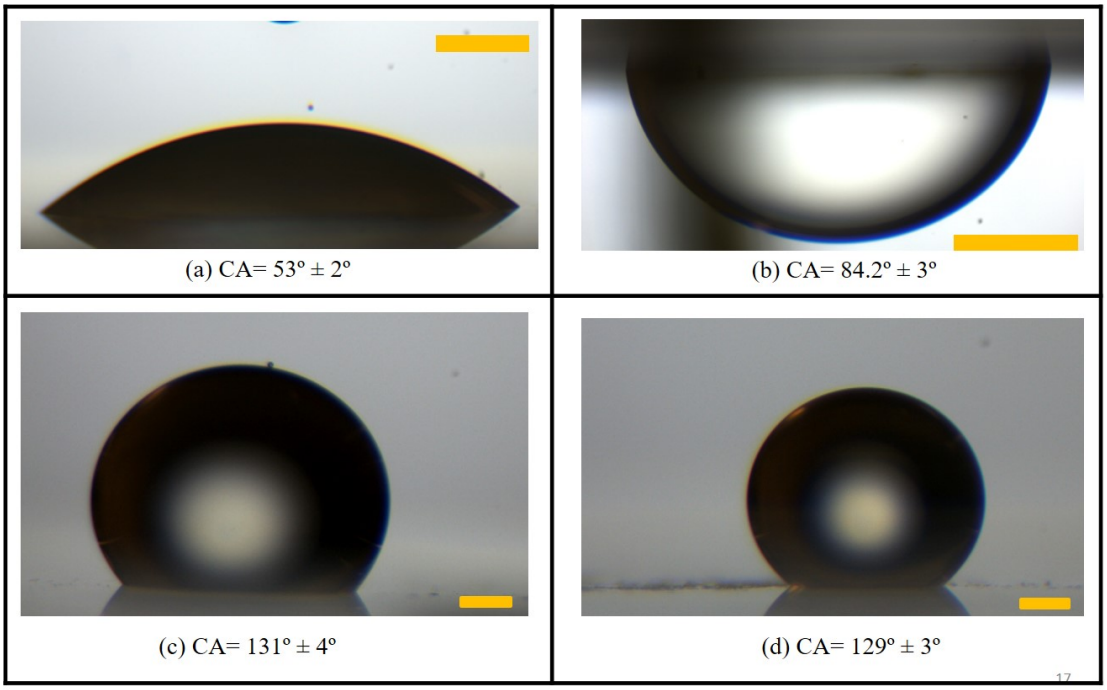

Figure 5.3: Optical images of different oil drops in water medium (a) DBP on PMMA (b) silicone oil-1 on PMMA (c) DBP on glass (d) laser oil on glass. The scale bar represents 1 mm.

of 87°±3°/74°±2°. Thus, we can see that DBP having a lower oil-water interfacial tension of 22.2 mN/m and viscosity of 16 mPa-s, showed smaller contact angle values on PMMA than laser oil that has a higher oil-water interfacial tension of 35.6 mN/m and viscosity of 130.4 mPa-s. Likewise, for silicone oil-1 (as shown in Fig. 5.3(b)) and silicone oil-2, the static equilibrium contact angles are 84.2°±3° and 86.8°±2°, respectively. Furthermore, silicone oil-1 and silicone oil-2 exhibited θ_A/θ_R of 105°±3°/83°±2.3° and 107°±3°/82°±2°, respectively.

However, we can see that silicone oil-2 with a higher viscosity of 484.6 mPa-s shows

only a slightly higher contact angle than silicone oil-1 with viscosity 48.1 mPa-s. This is due to the individual surface tensions and oil-water interfacial tension (Ref: Table 4.1), which are nearly the same for both the oils.

Table 5.3: Static and dynamic contact angles of oil (drop) in water (surrounding medium) on PMMA and glass substrates

Liquids	on PMMA Static CA	on PMMA θ_A/θ_R	on Glass Static CA	on Glass θ_A/θ_R
DBP	53°±2°	63°±2°/48°±3°	131°±4°	138°±3°/118°±2°
Laser oil	76°±4.5°	87°±3°/74°±2°	129°±3°	136°±2°/120°±1.5°
Silicone oil-1	84.2°±3°	105°±3°/83°±2.3°	166°±3°	172°±2°/158°±2.5°
Silicone oil-2	86.8°±2°	107°±3°/82°±2°	168°±3°	173°±2.1°/160°±1°

On the other hand, the static contact angles of DBP (drop) and laser oil (drop) on the underwater glass substrate are 131°±4° and 129°±3° (as illustrated in Fig. 5.3(c) and 5.3(d)), respectively. The advancing and receding contact angles, θ_A/θ_R of DBP and laser oil (drop) on the underwater glass substrate are 138°±3°/118°±2° and 136°±2°/120°±1.5°, respectively. Mitra and Mitra [20] reported static contact angles for DBP drop (121°), which is smaller than the observed value here and for laser oil drop (134°) on a glass substrate for a range of drop volume (2 - 7 μL). Also, Das et al. [16] and Waghmare et al. [15] reported that laser oil (drop) on the underwater glass substrate has contact angle in between 120° - 140° for a range of surfactant concentrations. Therefore, the observed values of contact angles are in good agreement with that available in literature. Static contact angle measurements of silicone oil-1 and silicone oil-2 are 166°±3° and 168°±3°, respectively. The θ_A/θ_R for both the oils are presented in Table 5.3. As such, one

can compare the contact angle values of oil (drop) in water medium on the two different substrates. PMMA showed an oleophilic nature than glass substrate with acute values of static contact angles (less than 90°). Whereas, for glass substrate, we observed an oleophobic nature with static contact angles greater that 125°.

5.1.3 Comparison of experimental and theoretical underliquid contact angles

5.1.3.1 Water (drop) in oil on PMMA

Table 5.4 illustrates the comparison between the observed (OCA_{wo}) and theoretical contact angle (TCA^{Y}) of water (drop) in oil medium on PMMA based on Young's equation (Refer Eq. 3.15). We can note that, with DBP as the surrounding oil medium, the percentage difference between the observed and the theoretical contact angle is only 9.59% while, the percentage difference found for water (drop) in other oils lies between 25.88% - 33.09%. The small difference with DBP as the surrounding fluid can be attributed due to hysteresis and surface roughness (AFM and Surface Profilometer studies are also performed and is discussed in chapter 3).

Thereafter, we applied the Owens and Wendt theory [34, 36, 37] by taking into account the polar and dispersive components of oils, water and substrate and calculated the contact angle. Accordingly, the contact angle for water (drop) in oil can be theoretically predicted with the Owens and Wendt theory by the Eq. 3.16. Table 5.5 presents that the percentage difference between the observed (OCA_{wo}) and the theoretical contact angle (TCA^{O-W}) of water (drop) in oils with Owens and Wendt theory. The percentage difference decreased from 25.88 % - 33.09% (Refer Table 5.4) to 8% - 20%. The smallest percentage difference

Table 5.4: Comparison of the observed (OCA) and theoretical contact angle (TCA) of water (drop) in oil on PMMA using Young's equation

Oil	OCA_{wo}	TCA^{Y}	%Difference $(OCA_{wo}\text{-}TCA^{Y})/OCA_{wo}$
DBP	146°±3°	132.1°±2°	9.59
Laser oil	136°±4°	100.8°±3°	25.88
Silicone oil-1	137°±4°	92.9°±2°	32.19
Silicone oil-2	139°±4.3°	93°±2°	33.09

observed is 8.09% with laser oil as the surrounding oil medium. However, with silicone oil-1 and silicone oil-2, the percentage difference observed is 16.06% and 20.43% respectively.

Table 5.5: Comparison of the observed (OCA) and theoretical contact angle (TCA) of water (drop) in oil on PMMA using Owens and Wendt theory

Oil	OCA_{wo}	TCA^{O-W}	%Difference $(OCA_{wo}\text{-}TCA^{O-W})/OCA_{wo}$
Laser oil	136°±4°	125°±3°	8.09
Silicone oil-1	137°±4°	115°±2°	16.06
Silicone oil-2	139°±4.3°	119.6°±2°	20.43

It is important to appreciate the difference in the wetting process that takes places in air medium (inviscid) in comparison to the one that takes place in presence of a viscous surrounding medium. In a related work, Mitra and Mitra [47] provided a theoretical framework of the drop coalescence on substrate kept in surrounding viscous medium. They derived a modified lubrication equation that takes into account the viscosity of the sur-

rounding liquid medium. More recently, Mitra and Mitra [20] also showed that underwater spreading of viscous oil drops in water medium is dominated by viscosity. Hence, it is evident that the surrounding viscous medium plays an important role to determine the wettability. We therefore, hypothesize about the possibility of a stable thin liquid film (originating from the surrounding medium) sandwiched between the droplet and the substrate that changes the wetting characteristics of the droplet. As mentioned earlier, in a related but for a very different problem, Daniel et al. [21] developed an experimental facility to measure nanometer thickness films using confocal Reflection Interference Contrast Microscopy (RICM) for understanding wetting of water drops floating on thin lubricating oil films. Such techniques can be used to observe the presence of any nanometer thick film beneath a droplet in underliquid system that might further elucidate the wetting signature.

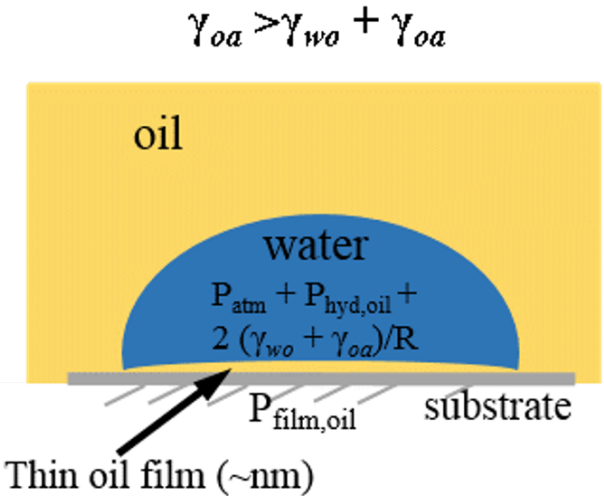

Figure 5.4: Schematic of pressure acting on thin oil film beneath the water drop in oil medium

In Figure 5.4, the water drop is pinned at a contact line on the substrate in the presence of a thin film of oil beneath the drop. According to Daniel et al. [21], $\gamma_{oa} > \gamma_{wo} + \gamma_{oa}$ when the droplet is covered by the lubricant film. This condition is true for the present work also, as the droplet is surrounded by oil medium. The Young-Laplace equation relates the curvature of a liquid interface to the pressure difference P between the two fluid phases. The pressure inside the droplet is $\mathrm{P}_{droplet} = P_{atm} + P_{hyd,oil} + 2(\gamma_{wo} + \gamma_{oa})/\mathrm{R}$, where P_{atm}= atmospheric pressure, $R \sim 1$mm is the radius of curvature, P_{hyd} is the hydrostatic pressure due to the height of oil as the surrounding liquid, wo and oa are oil/water and oil/air interfacial tensions respectively. Therefore, the pressure in the film, P_{film}=$P_{droplet}$. $\triangle$P $=2(\gamma_{wo} + \gamma_{oa})/\mathrm{R}$ is the driving pressure which squeezes the oil film up to a thickness of few nanometers.

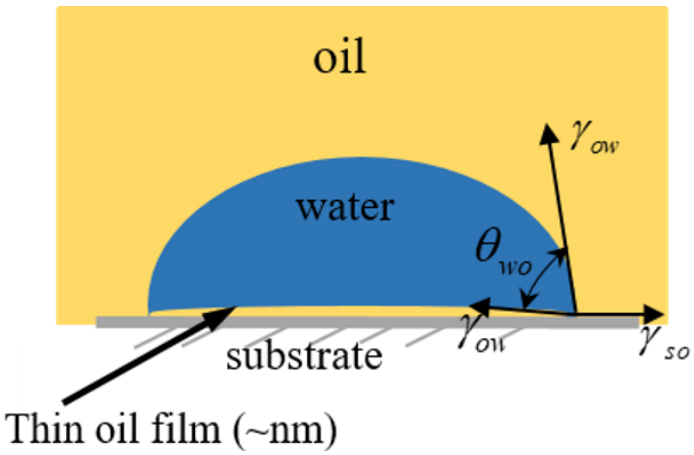

Figure 5.5: Schematic (not to scale) of water (drop) with thin oil film sandwiched between droplet and surrounding oil medium on a substrate

As conjectured, it is shown in Figure 5.5, a thin layer of oil (roughly nanometer in thickness) is present between the water droplet and substrate in the surrounding oil medium. Hence, we rewrite the Young's equation for water drop with a thin film of oil on the

substrate as

$$\gamma_{ow} + \gamma_{ow} cos\theta_{wo} = \gamma_{so} \tag{5.1}$$

Now, γ_{so} in Eq. 5.1 can be substituted from Eq. 3.13 (oil drop on a given substrate in air medium) to arrive at the simplified equation

$$\gamma_{ow} + \gamma_{ow} cos\theta_{wo} = \gamma_{sa} - \gamma_{oa} cos\theta_{oa}$$

We can rearrange the above equation as expressed below

$$\cos\theta_{wo} = \frac{(\gamma_{sa} - \gamma_{oa}\cos\theta_{oa} - \gamma_{ow})}{\gamma_{ow}} \tag{5.2}$$

Table 5.6 illustrates Young's equation with thin film consideration (Refer Eq.5.2), and the percentage difference between the observed (OCA_{wo}) and the theoretical contact angle ($\mathrm{TCA}^{Y}_{f,o}$) of water (drop) in silicone oil-1, silicone oil-2 and laser oil. We found that the percentage difference decreased from 8%-20% (Refer Table 5.5) to the range of 0.88% - 5.88%. Hence, this shows the likelihood of the formation of thin oil film beneath the water (drop) in the surrounding oil medium (laser oil, silicone oil-1, silicone oil-2). It is to be noted that silicone oil-1, which has a very small polar component ($\gamma^{p}_{oa} = 0.05\mathrm{mN/m}$), and the silicone oil-2, which is non polar ($\gamma^{p}_{oa} = 0\mathrm{mN/m}$), have a greater solid-oil interfacial tension and tends to form a thin oil film. Also, the percentage difference with laser oil as the surrounding medium is around 5.88% which may be due to contact angle hysteresis, surface roughness or even the contribution of its slightly higher polar component.

Table 5.6: Comparison of theoretical contact angle (TCA) and observed contact angle (OCA) of water drop in oil with thin oil film on PMMA substrate

Oil	OCA_{wo}	$TCA^{Y}_{f,o}$	%Difference $(OCA_{wo}\text{-}TCA^{Y}_{f,o})/OCA_{wo}$
Laser oil	136°±4°	144°±3°	5.88
Silicone oil-1	137°±4°	138.2°±2°	0.88
Silicone oil-2	139°±4.3°	142.7°±2°	2.66

5.1.3.2 Water (drop) in oil on glass

Similar to wetting on PMMA substrate, we tried to understand the wetting of water (drop) in oil medium on glass substrate where we found some key anomaly with the theoretical model for contact angle based on Young's equation. When experimentally observed contact angle values of oil and water on glass substrate in air medium are substituted in the Young's equation to determine equilibrium contact angle values for water (drop) in oil, (Eq. 3.15, section 3.1.4.1), we found that cos θ_{wo} is greater than +1. Similarly, when experimentally observed contact angle values of oil and water on glass substrate in air medium are substituted in the Young's equation to determine equilibrium contact angle values for oil (drop) in water, (Refer Eq. 3.18, section 3.1.4.3), we found that cos θ_{ow} is less than 1. Thus, the equation fail to satisfy the range of cosθ (cos θ_{ow} and cosθ_{wo}) which is [-1,1]. This is indeed surprising that over the years number of underliquid experimental contact angle values are reported in literature [13, 15, 19–21, 28, 29, 44], however, none have tried to compare with the theoretical models to reconcile them with the admissible range of the cosine function. However, the same equations are satisfied with PMMA as the substrate material. After comparisons we found that static contact angle of oil (drop) in air

medium on both PMMA and glass substrates lies in the same range (9° - 16°). But notable difference is the equilibrium contact angle for water (drop) in air medium on PMMA and glass substrates (76°±2° on PMMA and 14°±2° on glass). Therefore, governing parameter for the theoretical validity of equilibrium contact angles of the two-liquid system is the contact angle value of water (drop) in surrounding air medium. Hence, new investigations are necessary with modifications to the conventional governing theories by taking into account the surrounding viscous medium to accurately determine the theoretical wetting state.

Consequently, we considered the Owens and Wendt theory to predict the contact angle (Refer Eq. 3.16, section 3.1.4.2). Table 5.7 illustrates the percentage difference between the observed (OCA_{wo}) and the theoretical contact angle (TCA^{O-W}) of water (drop) in oil medium on a glass substrate using Owens and Wendt theory. We found that the percentage difference lies in the range of 36% - 79% and the smallest percentage difference was observed with DBP as the surrounding oil medium. We already mentioned that DBP does not form a thin oil film due to its high polar component and smaller solid/oil interfacial tension. Thus, it can be concluded that the other oils form a thin oil film beneath the water drop.

Table 5.7: Comparison of the observed (OCA) and theoretical contact angle (TCA) of water (drop) in oil on glass using Owens and Wendt theory

Oil	OCA_{wo}	TCA^{O-W}	%Difference (OCA_{wo}-TCA^{O-W})/OCA_{wo}
DBP	42°±3°	26.6°±2°	36.67
Laser oil	143°±2°	29.7°±3°	79.23
Silicone oil-1	96°±2°	31°±2°	67.71
Silicone oil-2	113°±2.5°	37.08°±2°	67.19

Therefore, we consider Young's equation with thin oil film (Eq. 5.2) to predict the contact angle for water (drop) in the oil medium on glass. Table 5.8 illustrates the percentage difference between the observed (OCA_{wo}) and the theoretical contact angle ($TCA^{Y}_{f,o}$) of water (drop) in laser oil, silicone oil-1 and silicone oil-2 as the surrounding oil medium on glass substrate. It was found that for silicone oil-1 and silicone oil-2, the percentage difference reduced to 3.85 % and 5.31 %. However, for laser oil, even though a significant reduction was observed, still we could find a percentage difference of 32.50%. The probable reason for this lack of agreement may be that the laser oil forms a partial film due to its slightly higher polar contribution compared to the silicone oils. For DBP, we observe that the percentage difference is 101.90%, which has increased from 36% on the basis of the Owens and Wendt theory. Therefore, one can conclude that DBP does not form a thin film between water drop and the glass substrate. We also observed a similar kind of behavior for a water drop on PMMA substrate in the surrounding DBP medium. This may be due to high polar component and smaller solid/oil interfacial tension of DBP.

Table 5.8: Comparison of theoretical contact angle (TCA) and observed contact angle (OCA) of water drop in oil with thin oil film on glass substrate using Young's equation

Oil	OCA_{wo}	$TCA^{Y}_{f,o}$	%Difference $(OCA_{wo}\text{-}TCA^{Y}_{f,o})/OCA_{wo}$
DBP	42°±3°	84.8°±3°	101.90
Laser oil	143°±2°	96.4°±2°	32.5
Silicone oil-1	96°±2°	99.7°±1°	3.85
Silicone oil-2	113°±2.5°	107°±1°	5.31

5.1.3.3 Oil (drop) in water on PMMA

For oil (drop) on the underwater PMMA substrate, we compared the experimentally observed contact angle (OCA_{ow}) with the theoretically calculated contact angle (TCA^Y) provided by Young's equation (Refer Eq. 3.18, section 3.1.4.3). Table 5.9 illustrates the comparison between observed and theoretical contact angle based on Young's equation. The percentage difference between the observed and the theoretical contact angle lies between 0.50% - 9.89%. The highest difference observed is for DBP with 9.89% which has a largest polar component ($\gamma_{oa}^p = 4.09$mN/m) of all the oils. Therefore, for oil drops on PMMA in presence of surrounding water medium, there is no formation of water film between the oil droplet and the PMMA substrate.

Table 5.9: Comparison of the observed (OCA) and theoretical contact angle (TCA) of oil (drop) in water on PMMA using Young's equation

Oil	OCA_{ow}	TCA^Y	%Difference $(OCA_{ow}\text{-}TCA^Y)/OCA_{ow}$
DBP	53°±3°	47.76°±2°	9.89
Laser oil	76°±4.5°	79.06°±3°	4.03
Silicone oil-1	84.2°±3°	86.95°±2°	3.27
Silicone oil-2	86.8°±2°	86.37°±2°	0.50

5.1.3.4 Oil (drop) in water on glass

As already discussed above, Young's equation (Refer Eq. 3.18, section 3.1.4.3) does not hold true to predict the contact angle oil (drop) in water medium on a glass substrate.

Therefore, we apply the standard Young's equation with a thin water film approximation as expressed below

As mentioned in Eq. 3.17 (section 3.1.4.3), Young's equation of an oil drop in water medium can be expressed as

$$\gamma_{so} + \gamma_{ow} cos\theta_{ow} = \gamma_{sw}$$

Now, as conjectured, we show in Figure 5.6, a thin layer of water (roughly nanometer in thickness) is present between the oil droplet and substrate in the surrounding water medium. Hence, we rewrite the equation for oil drop with a thin film of water on the substrate as

$$\gamma_{wo} + \gamma_{wo} cos\theta_{ow} = \gamma_{sw} \tag{5.3}$$

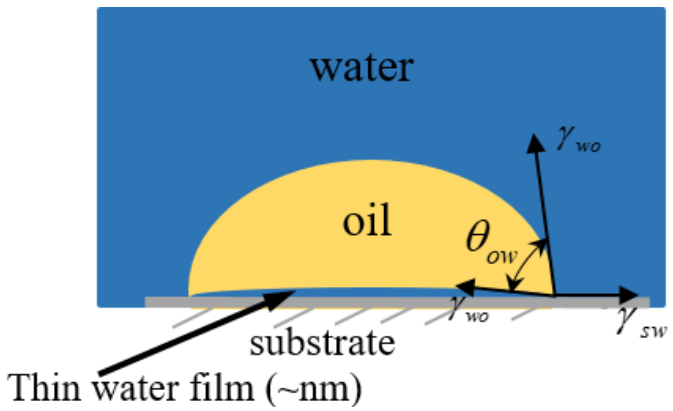

Figure 5.6: Schematic (not to scale) of oil (drop) with thin water film sandwiched between droplet and surrounding water medium on a substrate

Now, substituting γ_{sw} in Eq. 5.3 from Eq. 3.12 in section 3.1.4.1 (water droplet on a

given substrate in air) one can arrive at the simplified equation

$$\gamma_{wo} + \gamma_{wo} cos\theta_{ow} = \gamma_{sa} - \gamma_{wa} cos\theta_{wa}$$

$$\cos\theta_{ow} = \frac{(\gamma_{sa} - \gamma_{wa}\cos\theta_{wa} - \gamma_{ow})}{\gamma_{ow}} \tag{5.4}$$

After substituting the values in Eq. 5.4, we recalculated the contact angle for oil (drop) in water medium with a thin film of water for glass substrate. It was found that Young's equation with thin water film is still not valid to predict contact angles on a glass substrate. Hence, we considered the Owens and Wendt theory for oil (drop) in water medium with a thin water film, where we take all the polar and dispersive components of liquids as well as solids to predict the contact angle. Accordingly, we substitute γ_{sw} from Eq. 3.10 (section 3.4) to Eq. 5.3 (oil drop in water medium with a thin water film) to predict the contact angle and is expressed as

$$\cos\theta_{ow}^{O-W} = \frac{(\gamma_{sa} + \gamma_{wa} - 2(\gamma_{sa}^{d}\gamma_{wa}^{d})^{1/2} - 2(\gamma_{sa}^{p}\gamma_{wa}^{p})^{1/2} - \gamma_{ow})}{\gamma_{ow}} \tag{5.5}$$

Table 5.10: Comparison of observed (OCA) and theoretical contact angle (TCA) of oil (drop) in water on glass with thin film using Owens and Wendt theory

Oil	OCA_{ow}	$TCA_{f,w}^{O-W}$	%Difference (OCA_{ow}-$TCA_{f,w}^{O-W}$)/OCA_{ow}
DBP	131°±3°	163°±2°	24.43
Laser oil	129°±4.5°	167°±3°	29.46
Silicone oil-1	166°±3°	168°±2°	1.20
Silicone oil-2	168°±2°	169°±2°	0.60

Table 5.10 shows the comparison between the observed (OCA_{ow}) and theoretical contact angle ($TCA_{f,w}^{O-W}$) of oil (drop) in water medium based on the Owens and Wendt theory with the presence of a thin water film on the glass substrate. $TCA_{f,w}^{O-W}$ refers to the $\cos\theta_{ow}^{O-W}$ in Eq.5.5. The percentage difference between the observed and the theoretical contact angle is 0.60% for silicone oil-1 and 1.20% for silicone oil-2, respectively. The percentage difference observed for DBP and laser oil drop is in the range of 25%-30% on a glass substrate. This may be due to the very high polar contribution of the glass substrate ($\gamma_{oa}^{p} = 40\text{mN/m}$) that has an intermolecular attraction with the surrounding water medium and the polar oils.

Chapter 6

Conclusion and Future scope

The present work reports a first of its kind a detailed investigation of the wetting characteristics of oil (drop) in water medium and water (drop) in oil medium on under-liquid substrates. We have considered two model substrates - PMMA and glass, which are widely used by the wetting community and compared with the conventional theoretical model-Young's equation and Owens-Wendt approach. It is observed that in case of PMMA substrate, conventional theories do not translate to water (drop) in oil medium, however, it is not the case for oil drop in water medium for PMMA substrates. We therefore conjecture that there may be a thin oil film formed beneath the droplet that changes the wetting characteristics of the droplets, which leads to a difference in theoretical and experimental results. Accordingly, we presented a modified theoretical model based on Young's equation by considering a thin oil film originating from surrounding medium. After careful comparisons we observed that for water drop with surrounding medium of either of laser oil, silicone oil-1 and silicone oil-2 tend to form a thin oil film. However, DBP as surrounding oil medium do not form any film. This is due to the higher polar contribution

of DBP (γ_{oa}^{p} = 4.09mN/m). However, it is to be noted that silicone oil-1, which has a very small polar component (γ_{oa}^{p} = 0.05mN/m), and the silicone oil-2, which is non polar (γ_{oa}^{p} = 0mN/m) and therefore having a greater solid-oil interfacial tension tend to form a thin oil film. Laser oil as surrounding medium tends to form a partial film due to its slightly higher polar component (γ_{oa}^{p} = 0.62mN/m) than silicone oils.

Interestingly, the standard Young's equation do not translate to the under-liquid systems on a glass substrate. However, the modified Young's equation with thin oil film could predict the contact angle of water (drop) in oil on glass, showing the formation of thin oil film by silicone oil and silicone oil-2 and a partial film by laser oil. This behavior of laser oil is observed due to its slightly higher polar component (γ_{oa}^{p} = 0.62mN/m). Furthermore, Owens-Wendt approach with thin film of water beneath the oil drop is used to predict the under-water contact angle on glass substrate. It is observed that due to very high polar component of glass substrate (γ_{oa}^{p} = 40.28mN/m), water tends to form a thin film beneath oil drop of silicone oil-1 (γ_{oa}^{p} = 0.05mN/m) and silicone oil-2 (γ_{oa}^{p} = 0mN/m). Hence the present study eludes to the anomalous wetting behavior for under-liquid systems, which definitely demands well-defined experiments to decipher the three-phase contact line dynamics and visualize the thin film in presence of surrounding liquid media.

Hence, it is apparent that the natural future goal of this work is to visualize the thin film and to perform a detailed experimental validation of the present analysis for wetting signature of a drop in surrounding viscous medium. As such, experimental facility to measure nanometer thickness films using confocal reflection interference contrast microscopy can be used to observe the presence of any nanometer thick film beneath a droplet in an underliquid system and this might further elucidate the underliquid wetting signature.

References

(1) Gennes, P.-G.; Brochard-Wyart, F.; Quéré, D. Capillarity and Wetting Phenomena, Drops, Bubbles, Pearls, Waves. 2003.

(2) Bormashenko, E. Y., *Wetting of real surfaces*; Walter de Gruyter: 2013; Vol. 19.

(3) Joanny, J.; De Gennes, P.-G. *The Journal of Chemical Physics* **1984**, *81*, 552–562.

(4) Kuchin, I. V.; Starov, V. M. *Langmuir* **2016**, *32*, 5333–5340.

(5) Mitra, S.; Gunda, N. S. K.; Mitra, S. K. *RSC Advances* **2017**, *7*, 9064–9072.

(6) Eral, H.; Mannetje, D. J. C. M.; Oh, J. *Colloid and Polymer Science* **2013**, *291*, 247–260.

(7) Strobel, M.; Lyons, C. S. *Plasma Processes and Polymers* **2011**, *8*, 8–13.

(8) Tadmor, R.; Yadav, P. S. *Journal of Colloid and Interface Science* **2008**, *317*, 241–246.

(9) Bonn, D.; Eggers, J.; Indekeu, J.; Meunier, J.; Rolley, E. *Reviews of Modern Physics* **2009**, *81*, 739–805.

(10) Waghmare, P. R.; Gunda, N. S. K.; Mitra, S. K. *Scientific Reports* **2014**, *4*, 7454.

(11) De Gennes, P.-G.; Badoz, J. In *Fragile Objects*; Springer: 1996, pp 52–69.

(12) Bhushan, B. *Beilstein Journal of Nanotechnology* **2011**, *2*, 66–84.

(13) Jung, Y. C.; Bhushan, B. *Langmuir* **2009**, *25*, 14165–14173.

(14) Hejazi, V.; Nosonovsky, M. *Langmuir* **2011**, *28*, 2173–2180.

(15) Waghmare, P. R.; Das, S.; Mitra, S. K. *Scientific Reports* **2013**, *3*, 1862.

(16) Das, S.; Waghmare, P. R.; Fan, M.; Gunda, N. S. K.; Roy, S. S.; Mitra, S. K. *RSC Advances* **2012**, *2*, 8390–8401.

(17) Liu, M.; Wang, S.; Wei, Z.; Song, Y.; Jiang, L. *Advanced Materials* **2009**, *21*, 665–669.

(18) Goossens, S.; Seveno, D.; Rioboo, R.; Vaillant, A.; Conti, J.; Coninck, J. D. *Langmuir* **2011**, *27*, 9866–9872.

(19) Ozkan, O.; Erbil, H. Y. *Surface Topography: Metrology and Properties* **2017**, *5*, 024002.

(20) Mitra, S.; Mitra, S. K. *Langmuir* **2016**, *32*, 8843–8848.

(21) Daniel, D.; I, J. V.; Timonen; Li, R.; Velling, S. J.; Aizenberg, J. *Nature Physics* **2017**, *13*, 1020.

(22) Taniguchi, T.; Torii, T.; Higuchi, T. *Lab on a Chip* **2002**, *2*, 19–23.

(23) Seveno, D.; Blake, T.; Goossens, S.; De Coninck, J. *Langmuir* **2011**, *27*, 14958–14967.

(24) Bartell, F.; Osterhof, H. *Industrial & Engineering Chemistry* **1927**, *19*, 1277–1280.

(25) Van Dijke, M.; Sorbie, K. *Journal of Petroleum Science and Engineering* **2002**, *33*, 39–48.

(26) V Dijke, M.; Sorbie, K.; McDougall, S. *Advances in Water Resources* **2001**, *24*, 365–384.

(27) Grate, J. W.; Dehoff, K. J.; Warner, M. G.; Pittman, J. W.; Wietsma, T. W.; Zhang, C.; Oostrom, M. *Langmuir* **2012**, *28*, 7182–7188.

(28) Fetzer, R.; Ramiasa, M.; Ralston, J. *Langmuir* **2009**, *25*, 8069–8074.

(29) Ramiasa, M.; Ralston, J.; Fetzer, R.; Sedev, R. *The Journal of Physical Chemistry C* **2011**, *115*, 24975–24986.

(30) Goswami, A.; Bhagwat, S. S. *Tenside Surfactants Detergents* **2015**, *52*, 245–251.

(31) Good, R. J.; Girifalco, L. *The Journal of Physical Chemistry* **1960**, *64*, 561–565.

(32) Girifalco, L.; Good, R. J. *The Journal of Physical Chemistry* **1957**, *61*, 904–909.

(33) Fowkes, F. M. *Industrial & Engineering Chemistry* **1964**, *56*, 40–52.

(34) Owens, D. K.; Wendt, R. *Journal of applied polymer science* **1969**, *13*, 1741–1747.

(35) Rulison, C. *A tutorial designed to provide basic understanding of the concept solid surface energy, and its many complications, TN306/CR* **1999**, 1–16.

(36) Binks, B. P.; Tyowua, A. T. *Soft Matter* **2016**, *12*, 876–887.

(37) Binks, B. P.; Clint, J. H. *Langmuir* **2002**, *18*, 1270–1273.

(38) Voinov, O. *Fluid Dynamics* **1976**, *11*, 714–721.

(39) Cox, R. G. *Journal of Fluid Mechanics* **1986**, *168*, 169–194.

(40) Tanner, L. H. *Journal of Physics D: Applied Physics* **1979**, *12*, 1473–1484.

(41) Cazabat, A. M.; Valignat, M. P.; Villette, S.; Coninck, J. D.; Louch, F. *Langmuir* **1997**, *13*, 4754–4757.

(42) Extrand, C. W. *Langmuir* **2016**, *32*, 7697–7706.

(43) De Ruijter, M. J.; Charlot, M.; Voué, M.; De Coninck, J. *Langmuir* **2000**, *16*, 2363–2368.

(44) Svitova, T.; Theodoly, O.; Christiano, S.; Hill, R.; Radke, C. *Langmuir* **2002**, *18*, 6821–6829.

(45) Fort Jr, T.; Patterson, H. *Journal of Colloid Science* **1963**, *18*, 217–222.

(46) Carroll, B. *Journal of Colloid and Interface Science* **1976**, *57*, 488–495.

(47) Mitra, S.; Mitra, S. K. *Physical Review E* **2015**, *92*, 033013.